ACTA ODONTOLOGICA SCANDINAVICA
2022, VOL. 80, NO. 2, 140–149
https://doi.org/10.1080/00016357.2021.1964593

Taylor & Francis
Taylor & Francis Group

ORIGINAL ARTICLE

miR-200a-3p represses osteogenesis of human periodontal ligament stem cells by targeting ZEB2 and activating the NF-κB pathway

Qing Wang[a]*, Haiyan Lin[a]*, Jinxiang Ran[b], Ziran Jiang[c], Qingyuan Ren[a], Wulin He[a] and Hui Xiao[a]

[a]Department of Orthodontics, Stomatological Hospital, Southern Medical University, Guangzhou, China; [b]Department of Orthodontics, Qiannan Traditional Chinese Medical Hospital, School of Stomatology and Medicine, Qiannan Buyi and Miao Autonomous Prefecture, Duyun, China; [c]Department of Orthodontics, Foshan Stomatology Hospital, School of Stomatology and Medicine, Foshan, China

ABSTRACT

Objectives: Human periodontal ligament stem cells (hPDLSCs) bear multilineage differentiation potential and represent the cytological basis of periodontal tissue regeneration. microRNA (miR) is accepted as a critical regulator of cell differentiation. This study explored the molecular mechanism of miR-200a-3p in osteogenesis of hPDLSCs.

Material and methods: hPDLSCs were cultured and identified *in vitro*. miR-200a-3p expression during osteogenic differentiation of hPDLSCs was detected. hPDLSCs were transfected with miR-200a-3p mimic or miR-200a-3p inhibitor. Alkaline phosphatase (ALP) activity, calcified nodules and osteogenesis-related genes of hPDLSCs were measured. The binding relationship between miR-200a-3p and ZEB2 was predicted and verified. hPDLSCs were infected with sh-ZEB2, and then the osteogenic capacity was examined. miR-200a-3p inhibitor-transfected hPDLSCs were infected with sh-ZEB2. The key proteins of the NF-κB pathway were measured.

Results: miR-200a-3p expression was downregulated during osteogenic differentiation of hPDLSCs. Upregulation of miR-200a-3p reduced ALP activity, calcified nodules and osteogenesis-related genes of hPDLSCs, while downregulation of miR-200a-3p facilitated the osteogenesis of hPDLSCs. miR-200a-3p targeted ZEB2. ZEB2 silencing repressed osteogenesis of hPDLSCs. ZEB2 silencing attenuated the promoting effect of miR-200a-3p inhibitor on osteogenesis of hPDLSCs. miR-200a-3p activated the NF-κB pathway by targeting ZEB2.

Conclusion: miR-200a-3p repressed osteogenesis of hPDLSCs by targeting ZEB2 and activating the NF-κB pathway. This study may offer insights for periodontal tissue regeneration engineering.

ARTICLE HISTORY
Received 4 June 2021
Revised 20 July 2021
Accepted 24 July 2021

KEYWORDS
Osteogenesis; miR-200a-3p; ZEB2; human periodontal ligament stem cells; NF-κB pathway; molecular mechanism

Introduction

Periodontium is composed of root cementum, alveolar bone, gingiva and periodontal ligament (PDL), with the main functions of supporting and protecting the tooth, nerve and blood vessels from mechanical loading-caused injury [1]. PDL is a soft connective tissue between cementum and inner wall of alveolar bone, which can maintain teeth *in situ*, keep tissue homoeostasis and repair injured periodontal tissues [2]. In 2004, Seo *et al.* first elucidated that PDL has stem cells that may produce cementum/PDL-like tissues *in vivo* and termed them human periodontal ligament stem cells (hPDLSCs) [3]. hPDLSCs bear multilineage differentiation potential and contribute to the physiological healing of cementum-PDL complex and alveolar bone [4], which are commonly accepted as promising stem cells for periodontal regeneration therapy [1,2]. Despite the immerse interest in hPDLSC-based therapies, the clinical application of hPDLSCs is confined by the deficient understanding of the molecular mechanisms underlying their directional differentiation. Hence, elucidating the potential mechanism of osteogenesis of hPDLSCs has practical significance for periodontal regeneration therapy.

microRNAs (miRs) are highly conserved endogenous non-protein RNAs, which modulate cell proliferation, differentiation and apoptosis *via* binding to the 3′ untranslated region of target mRNAs [5]. miRs are implicated in the osteogenesis of hPDLSCs by suppressing the mRNA or protein level of target genes, and consequently miR-based therapy possesses crucial values in facilitating periodontal tissue repair and regeneration [6]. For example, Xue *et al.* have revealed that miR-125b represses osteogenesis of hPDLSCs by targeting NKIRAS2 [7]. Wei *et al.* have exhibited that elevated miR-21 expression can restrain osteogenesis of hPDLSCs by targeting Smad5 [8]. miR-200, a family of tumour suppressor miRs, is implicated in the suppression of epithelial–mesenchymal transition, repression of cancer stem cells self-renewal and differentiation, and reversal of chemoresistance [9]. miR-200a-3p belongs to the miR-200 family and locates on chromosome 1p36, which is reported to modulate human cancer progression [10]. Notably, miR-200a-3p represses the osteogenesis of bone marrow mesenchymal stem cells

CONTACT Hui Xiao huix0628@163.com; Wulin He lanxun83417@163.com Department of Orthodontics, Stomatological Hospital, Southern Medical University, NO. 366 South Jiangnan Avenue, Haizhu District, Guangdong, 510280, China
*Theese authors are co-first authors.

(BMSCs) by targeting glutaminase, thereby accelerating the progress of osteoporosis [11]. However, the molecular mechanism of miR-200a-3p in the osteogenesis of hPDLSCs remains unclear. This study herein investigated the role of miR-200a-3p in the osteogenesis of hPDLSCs, along with its downstream mechanism, which shall provide a theoretical basis for the management of periodontal regeneration.

Materials and methods

Ethics statement

The study got the approval of the Clinical Ethical Committee of Stomatological Hospital, Southern Medical University.

Identification and culture of hPDLSCs

Fresh premolars without any caries were extracted from the healthy individual aged 18–23 old due to orthodontics. The PDL tissues were gently scraped from the middle one-third of the root to prevent the contamination of gingival and cementum cells. The tissues were cut into small pieces and placed in a 35-mm culture dish for cell transplantation. The cells were cultured in Dulbecco's modified Eagle's medium (DMEM) containing 10% foetal bovine serum (FBS; 10270, Gibco, Grand Island, NY, USA), 2 mM L-glutamine (35050, Gibco), 100 U/mL penicillin, 100 μg/mL streptomycin and 250 μg/mL amphotericin B (Antibiotic-Antimycotic; 15240, Gibco) at 37 °C with 5% CO_2 and saturated humidity. The medium was refreshed every 48 h. Cells were passaged at 1:3 until reaching 70% confluence.

Osteogenic induction of hPDLSCs

The well-grown hPDLSCs at passage 3–6 were detached with trypsin, centrifuged and collected. Then, cells were seeded into 24-well plates (75000 cells/well) and kept in the growth medium for 24 h. Next, the growth medium was replaced with osteogenic medium containing 50 μg/mL ascorbic acid (A-4034, Sigma-Aldrich, Merck KGaA, Darmstadt, Germany), 250 nM dexamethasone (D8893, Sigma-Aldrich), and 5 mM β-glycerophosphate (G9422, Sigma-Aldrich). The control cells were cultured in DMEM for 21 d. The medium was refreshed every 3–4 d. Cell morphology was observed under an inverted microscope.

Cell transfection

miR-200a-3p mimic and its negative control mimic-NC, miR-200a-3p inhibitor and its negative control inhibitor-NC were designed and synthesised by Guangzhou RiboBio Co., Ltd (Guangzhou, Guangdong, China). When the cell confluence reached 70%, hPDLSCs were cultured overnight in α-MEM medium free of penicillin and streptomycin. The next day, the mimics or inhibitors were transfected into hPDLSCs using the Lipofectamine™ 3000 (Thermo Fisher Scientific Inc., Waltham, MA, USA). EP. 1 tube was added with 250 μL medium and 5 μL miR-200a-3p mimic, miR-200a-3p inhibitor, mimic NC and inhibitor NC, respectively, and was kept for 5 min. EP. 2 tube was added with 250 μL medium and 5 μL Lipofectamine™ 3000. After 5 min, the two EP tubes were mixed evenly, added into the 6-well plates after standing for 20 min, and cultured in the incubator containing 5% CO_2 at 37 °C. After 6 h, cells were cultured in DMEM. The subsequent experiment was carried out after 24 h. To ensure the efficiency of transfection, cells are transfected once every 3 days.

Lentiviral vector of ZEB2 (shRNA-ZEB2) was purchased from Shanghai GenePharma Co., Ltd (Shanghai, China). The multiplicity of infection was 20. The cells in sh-NC group were transfected with blank lentiviral vector to serve as the control. On the day before transfection, hPDLSCs in the logarithmic phase at passage 3 were seeded into 24-well plates (1×10^6 cells/mL). The cells were infected with adjusted lentivirus when reaching 70% confluence. After 12 h of infection, the cells were further cultured in the complete medium. The cells were passaged for cell experiment at 48 h post virus infection. The joint experiment of shRNA-ZEB2 and *miR-200a-3p* inhibitors was performed by the transfection of miR-200a-3p inhibitor after 48 h of the transfection of lentiviral vector ZEB2 (shRNA-ZEB2).

Alkaline phosphatase (ALP) staining

After 21 d of osteogenic induction, the original culture medium was removed. The cells were washed with phosphate-buffered saline (PBS; Sigma-Aldrich) 2–3 times and fixed with 10% formalin for 10 min. Following PBS washing, the cells were stained with BCIP/NBT (Roche Diagnostics, Indianapolis, IN, USA) for 30 min in the dark. The cells were observed and photographed under the inverted microscope. The cells in each well were treated with cell lysate (002201, Life Technologies, Gaithersburg, MD, USA). The ultrasonic cell disrupter (Branson Ultrasonics (Shanghai) Co., Ltd., Shanghai, China) was used to promote the protein release. Subsequently, the cells were centrifuged at 4 °C and 15000 rpm to collect the supernatants, supplemented with buffer and cultured at 37 °C for 15–30 min. Then, 0.1 M NaOH was added to terminate the reaction. The absorbance value at 405 nm was determined using a microplate Reader (BioTek Instruments Inc., Winooski, VT, USA).

Alizarin red S staining

After 21 d of osteogenic induction, the original culture medium was removed. The cells were washed with PBS (Sigma-Aldrich) 2–3 times and fixed with 4% paraformaldehyde (Sigma-Aldrich) for 10 min. Following washing in deionized water, the cells were stained with 2% alizarin red solution (Santa Cruz Biotechnology, Inc, Santa Cruz, CA, USA) for 15 min. The calcified nodules were observed and photographed under the inverted microscope. The absorbance value at 570 nm was measured using a microplate Reader (BioTek) to determine the relative content of calcified nodules.

Table 1. Primer sequence for RT-qPCR.

Gene	Sequences (5′-3′)
miR-200a-3p-F	CCTACGCCACAATTAACAAGCC
miR-200a-3p-R	GCCGTCTAACACTGTCTGGTA
U6-F	ATTGGAACGATACAGAGAAGATT
U6-R	GGAACGCTTCACGAATTTC
ZEB2-F	CCTGCCTCACTAAACCCACA
ZEB2-R	CCTTGTTCCTGTGCTTGGCAT
Runx2-F	AGCTTCTGTCTGTGCCTTCTGG
Runx2-R	GGAGTAGAGAGGCAAGAGTTT
OCN-F	CCCAGGCGCTACCTGTATCAA
OCN-R	GGTCAGCCAACTCGTCACAGTC
OPN-F	GCCGACCAAGGAAAACTCACT
OPN-R	GGCACAGGTGATGCCTAGGA
ALP-F	GGACCATTCCCACGTCTTCAC
ALP-R	CCTTGTAGCCAGGCCCATTG
β-actin-F	TGGCACCCAGCACAATGAA
β-actin-R	CTAAGTCATAGTCCGCCTAGAAGCA
Lamin A-F	GTCGATGAAGAGGGAAAGTT
Lamin A-R	AAAGGATCGTCACCATTCTG

Note: Runx2, Runt-related transcription factor 2; OPN, osteopontin; OCN, osteocalcin; ALP, Alkaline phosphatase.

Reverse transcription quantitative polymerase chain reaction (RT-qPCR)

Total RNA of hPDLSCs was extracted using TRIzol reagent (Ambion, Austin, TX, USA) and reverse transcribed into cDNA using the PrimeScript RT kit (Takara Bio Inc., Kyoto, Japan). RT-qPCR was conducted using SYBR® Premix Ex Taq™ II kit (Takara) and quantitative PCR instrument (ABI 7500, Applied Biosystems, Inc., Carlsbad, CA, USA). Relative expression of genes was examined by $2^{-\Delta\Delta Ct}$ method, with Lamin A and β-actin as the internal reference. The primers are shown in Table 1.

Dual-luciferase reporter gene assay

The binding site between miR-200a-3p and ZEB2 was predicted by Targetscan (http://www.targetscan. org). The binding sequence and mutation sequence of miR-200a-3p and ZEB2 were amplified and cloned into the downstream of psiCHECK-2 plasmid containing luciferase (Beijing TianGen Biotech Co., Ltd, Beijing, China). The wild-type (WT) vector (ZEB2-WT) and the mutant type (MUT) vector (ZEB2-MUT) were constructed. mimic-NC and *miR-200a-3p* mimic were co-transfected into hPDLSCs using the Lipofectamine™ 3000 (Thermo Fisher). The luciferase activity was detected after 48 h.

Western blotting

hPDLSCs were lysed in radio-immunoprecipitation assay buffer (Beyotime Biotechnology Co., Ltd, Shanghai, China). The protein concentration was tested using the Pierce™ bicinchoninic acid assay kit (Thermo Fisher). The protein was separated on 12% SDS-PAGE and transferred onto polyvinylidene fluoride membranes. The membranes were cultured with the primary antibodies at 4 °C for 24 h. Following tris-buffered saline-tween (TBST) washing three times, the membranes were cultured with the secondary antibody mouse anti-human Vimentin (ZSGB-BIO, Beijing, China). Next, the protein bands were developed and visualized using the Novex enhanced chemiluminescence reagent (Invitrogen Inc., Carlsbad, CA, USA). The grey value of each band was quantified using Image Pro Plus 6.0 (Media Cybernetics, Silver Spring, MD, USA). β-actin and GAPDH were used as the internal control of cytoplasmic protein and Lamin A was used as the internal control of nuclear protein. Each experiment was repeated three times. The primary antibodies are shown in Table 2.

Table 2. The primary antibodies used in Western blotting.

Primary antibody	Dilution ratio	cat. no.	Company
ZEB2	1:500	ab230561	Abcam, UK
IκB	1:10000	ab32518	Abcam, UK
pIκB	1:2000	ab239920	Cell Signalling, USA
p65	1:2000	ab16502	Abcam, UK
Runx2	1:1000	ab236639	Cell Signalling, USA
ALP	1:1000	ab154100	Abcam, UK
OPN	1:1000	ab228748	Abcam, UK
OCN	1:5000	ab133612	Abcam, UK
Lamin A	1:5000	ab108595	Abcam, UK
β-actin	1:5000	ab8227	Abcam, UK
GAPDH	1:100	ab8245	Abcam, UK

Statistical analysis

Data analysis was introduced using the SPSS 21.0 (IBM Corp., Armonk, NY, USA) and GraphPad Prism 8.0.1 (GraphPad Software, San Diego, CA, USA). Data are expressed as mean ± standard deviation. Kolmogorov–Smirnov method was adopted to check whether the data were in normal distribution. If the data were in normal distribution and homogeneity of variance, then the *t*-test was adopted for comparison between two groups. One-way analysis of variance (ANOVA) or two-way ANOVA was employed for the comparisons among multiple groups, following Tukey's multiple comparisons test. If the data were not in normal distribution or homogeneity of variance, the rank-sum test was carried out. The $p < .05$ meant a statistically significant.

Results

Overexpression of miR-200a-3p inhibited osteogenesis of hPDLSCs

miR-200a-3p represses osteogenesis of BMSCs by targeting glutaminase, thus accelerating the progress of osteoporosis [11]. miR-200a-3p expression during osteogenic differentiation of hPDLSCs was detected. miR-200a-3p expression in hPDLSCs was downregulated from the first day after cultured in osteogenic differentiation medium for 0, 3, 7 and 14 days, and reached the lowest level after 14 days (all $p < .05$; Figure 1(A)). Then, hPDLSCs were transfected with miR-200a-3p mimic or miR-200a-3p inhibitor. miR-200a-3p expression in hPDLSCs was promoted 24 h after miR-200a-3p mimic transfection and significantly reduced 24 h after miR-200a-3p inhibitor transfection (all $p < .05$; Figure 1(B)). After 21 days of osteogenic induction, miR-200a-3p mimic-transfected hPDLSCs showed reduced ALP activity and lessened number and volume of calcified nodules, while miR-200a-3p inhibitor-

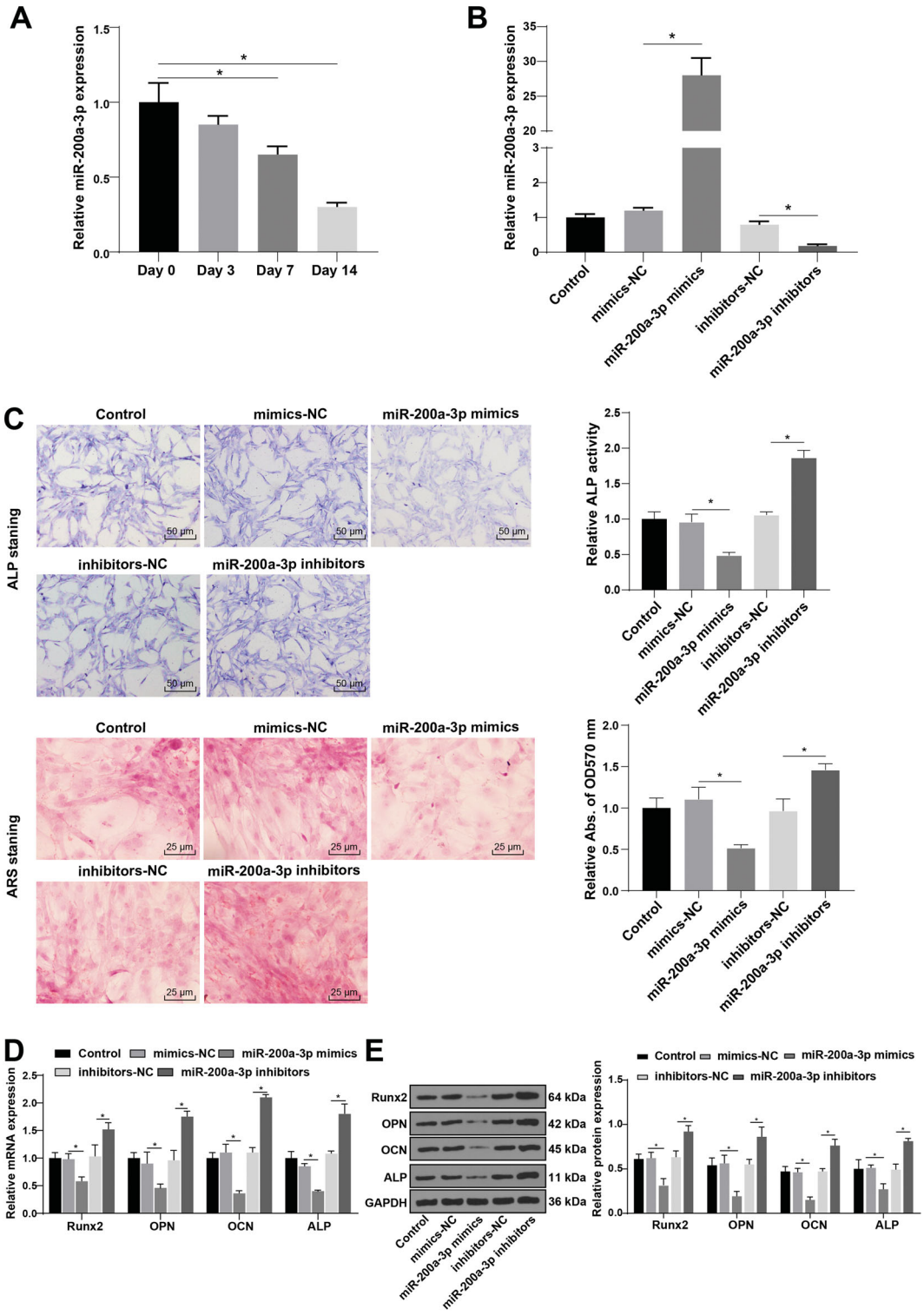

Figure 1. Overexpression of miR-200a-3p inhibited osteogenesis of hPDLSCs. A: miR-200a-3p expression during osteogenic differentiation of hPDLSCs was detected using RT-qPCR. hPDLSCs were transfected with miR-200a-3p mimic or miR-200a-3p inhibitor. B: miR-200a-3p expression in hPDLSCs at 24 h after transfection was detected using RT-qPCR; C: ALP activity and calcified nodules were measured using ALP staining and alizarin red staining; D–E: levels of osteogenesis-related genes (Runx2, OPN, OCN and ALP) were detected using RT-qPCR and Western blotting. The cell experiment was repeated three times independently. Data are presented as mean ± standard deviation and analysed using one-way ANOVA or two-way ANOVA, followed by Tukey's multiple comparisons test, $^{*}p < .05$.

transfected hPDLSCs had an opposite trend (all $p < .05$; Figure 1(C)). The levels of osteogenesis-related genes (Runx2, OPN, OCN and ALP) were also measured using RT-qPCR and Western Blot (WB). The levels of these genes were downregulated in miR-200a-3p mimic-transfected hPDLSCs compared with the mimic NC-transfected cells but were upregulated in miR-200a-3p inhibitor-transfected hPDLSCs compared with the inhibitor NC-transfected cells (all $p < .05$; Figure 1(D/E)). Briefly, overexpression of miR-200a-3p repressed osteogenesis of hPDLSCs.

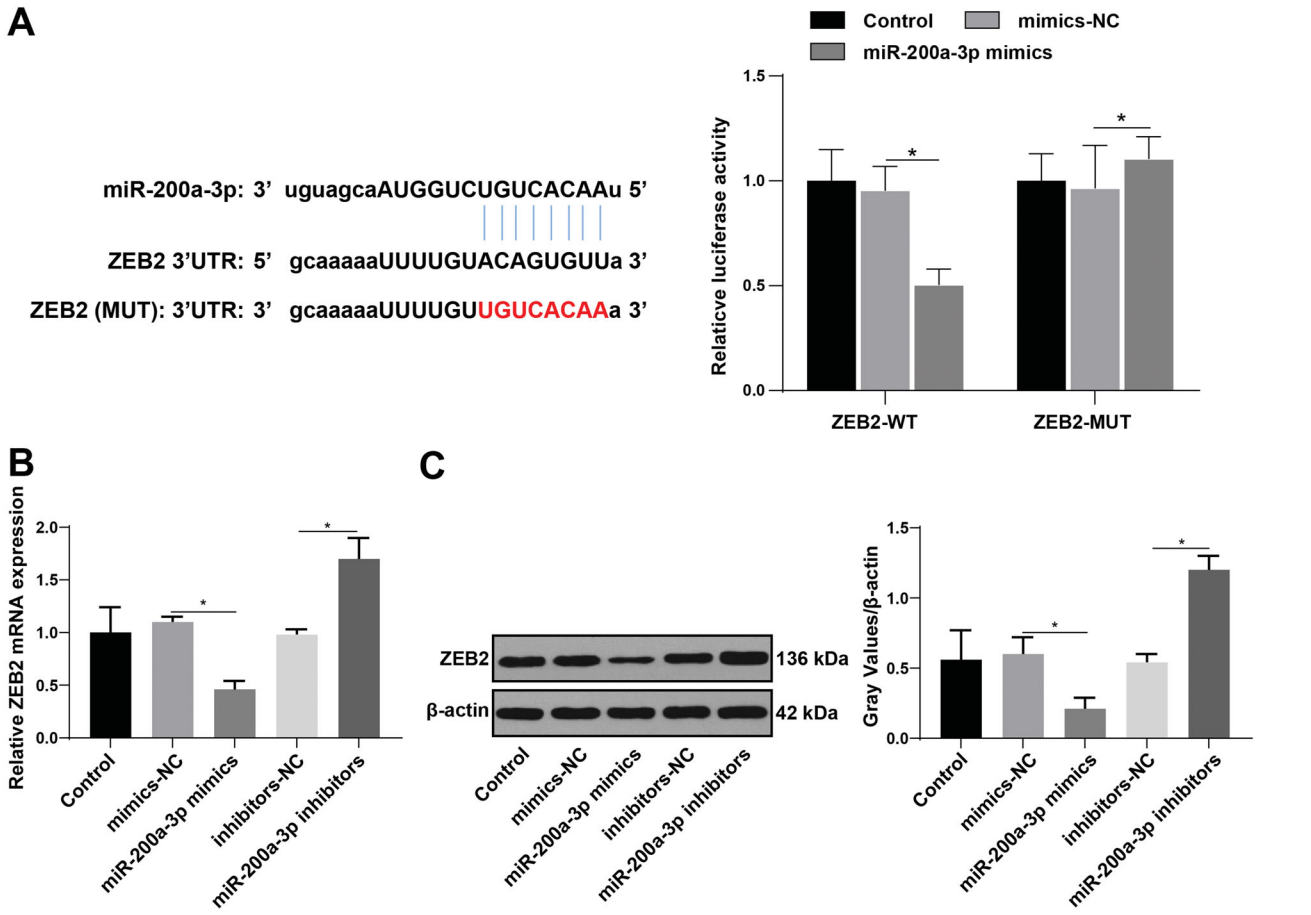

Figure 2. miR-200a-3p targeted ZEB2. A: the binding relationship between miR-200a-3p and ZEB2 was verified using dual-luciferase reporter gene assay; mRNA and protein levels of ZEB2 in hPDLSCs transfected with miR-200a-3p mimic or miR-200a-3p inhibitor were detected using RT-qPCR (B) and Western blotting (C). The cell experiment was repeated three times independently. Data are presented as mean ± standard deviation and analysed using one-way ANOVA or two-way ANOVA, followed by Tukey's multiple comparisons test, $^{*}p < .05$.

miR-200a-3p targeted ZEB2

We then explored the molecular mechanism of miR-200a-3p regulating osteogenesis of hPDLSCs. Bioinformatics software (http://www.targetscan.org) showed that miR-200a-3p has binding sites with 3′-UTR of ZEB2. ZEB2 has been demonstrated to attenuate the osteogenic differentiation defects in diabetic osteoporosis [12]. The binding relationship between miR-200a-3p and ZEB2 was verified using dual-luciferase reporter gene assay (all $p < .05$; Figure 2(A)). The mRNA and protein levels of ZEB2 were notably declined in miR-200a-3p mimic-transfected hPDLSCs, but promoted in miR-200a-3p inhibitor-transfected hPDLSCs (all $p < .05$; Figure 2(B/C)). miR-200a-3p targeted ZEB2 in hPDLSCs.

Silencing ZEB2 inhibited osteogenesis of hPDLSCs

Based on the above results, we then verified the relationship between ZEB2 and osteogenesis. hPDLSCs were infected with sh-ZEB2 for 2 days and cultured in osteogenic differentiation medium for 21 days. ZEB2 expression in hPDLSCs in the sh-ZEB2 group was notably downregulated compared with that in the sh-NC group (all $p < .05$; Figure 3(A)). hPDLSCs in the sh-ZEB2 group showed decreased ALP activity and reduced number and volume of calcified nodules (all $p < .05$; Figure 3(B)). Additionally, RT-qPCR and WB demonstrated that the levels of osteogenesis-related genes of hPDLSCs in the sh-ZEB2 group were notably reduced (all $p < .05$; Figure 3(C/D)). Taken together, silencing ZEB2 repressed osteogenesis of hPDLSCs.

miR-200a-3p inhibited osteogenesis of hPDLSCs by targeting ZEB2

Functional rescue experiment was conducted to verify that miR-200a-3p repressed osteogenesis of hPDLSCs by targeting ZEB2. hPDLSCs in the miR-200a-3p inhibitor group were infected with sh-ZEB2. RT-qPCR demonstrated that compared with the sh-NC + *miR-200a-3p* inhibitor group, the expression of ZEB2 was downregulated in the sh-ZEB2 + *miR-200a-3p* inhibitor group, indicating that the co-transfection was successful ($p < .05$, Figure 4(A)). Furthermore, hPDLSCs in the sh-ZEB2 + miR-200a-3p inhibitor group showed reduced ALP activity, calcified nodules and osteogenesis-related genes, compared with hPDLSCs in the sh-NC + miR-200a-3p inhibitor group (all $p < .05$; Figure 4(B–D)). It was confirmed that

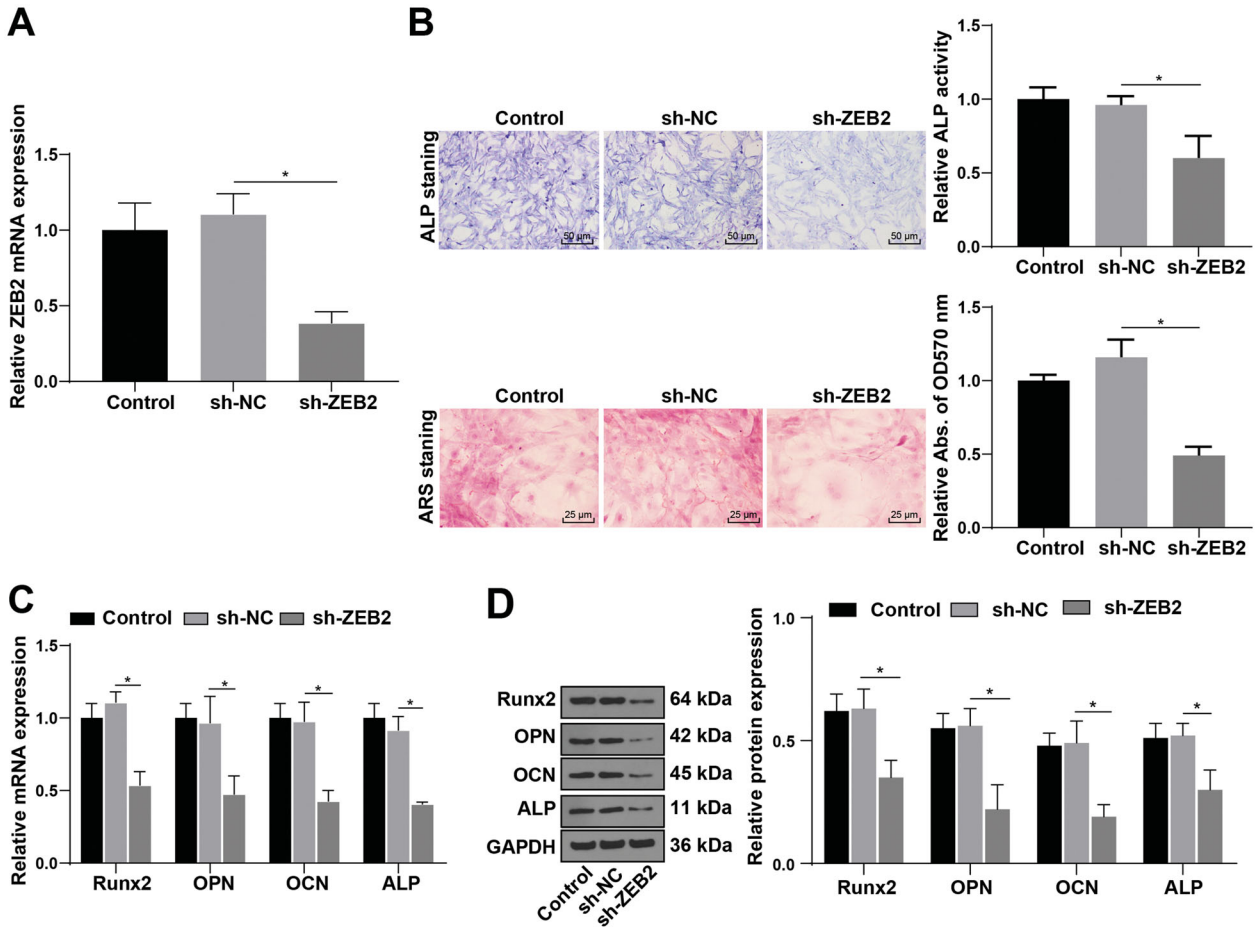

Figure 3. ZEB2 silencing inhibited osteogenesis of hPDLSCs. hPDLSCs were infected with sh-ZEB2 for 2 days and cultured in osteogenic differentiation medium for 21 days. **A:** ZEB2 expression in hPDLSCs was detected using RT-qPCR; B: ALP activity and calcified nodules were measured using ALP staining and alizarin red staining; C-D: levels of osteogenesis-related genes (Runx2, OPN, OCN and ALP) were detected using RT-qPCR and Western blotting. The cell experiment was repeated three times independently. Data are presented as mean ± standard deviation and analysed using one-way ANOVA or two-way ANOVA, followed by Tukey's multiple comparisons test, $^*p < .05$.

miR-200a-3p suppressed osteogenesis of hPDLSCs by targeting ZEB2.

miR-200a-3p activated the NF-κB signalling pathway by targeting ZEB2

ZEB2 can reduce the inflammation of HK-2 cells induced by lipopolysaccharide (LPS) *via* the NF-κB pathway, which indicates that ZEB2 inactivates the NF-κB pathway [13]. The activation of NF-κB pathway was mainly manifested by translocation of p50 (NFKB1)/p65 (RelA) (i) and p50/p65 to nucleus (ii) and interaction between p50/p65 and its target gene (iii). We then investigated whether miR-200a-3p could regulate the NF-κB pathway by targeting ZEB2 during osteogenesis of hPDLSCs. The key proteins of the NF-κB pathway in sh-ZEB2-infected cells were detected. After sh-ZEB2 infection, IκB and p65 protein levels in the cytoplasm were decreased and pIκB protein level was increased, and p65 protein level in nucleus was increased (all $p < .05$; Figure 5(A)). It was suggested that ZEB2 silencing promoted p65 into the nucleus of hPDLSCs. Additionally, miR-200a-3p mimic-transfected hPDLSCs showed decreased IκB and p65 protein levels in cytoplasm but increased p65 protein level in the nucleus, while miR-200a-3p inhibitor-transfected hPDLSCs had the opposite trend (all $p < .05$; Figure 5(B)). Overall, miR-200a-3p repressed osteogenesis of hPDLSCs by targeting ZEB2 and activating the NF-κB pathway.

Discussion

The discovery of hPDLSCs highlights the promising potential for the application of tissue engineering-based therapies for destructed periodontium [1,2]. The osteogenesis ability enables hPDLSCs to be a potential target for the promotion of functional restoration of periodontal tissues [14]. miR-200a-3p is reported to inhibit the osteogenesis of BMSCs [11]. This study revealed that overexpression of miR-200a-3p repressed osteogenesis of hPDLSCs *via* the ZEB2/NF-κB axis.

The regeneration and repair of periodontal tissues mainly depend on the osteogenesis capacity of hPDLSCs [15]. Emerging evidence has revealed that altered miR expression is implicated in the osteogenesis of hPDLSC [8,16,17]. In the current study, RT-qPCR demonstrated that miR-200a-3p expression was reduced during the osteogenesis of hPDLSCs. Then hPDLSCs were transfected with miR-200a-3p mimic or miR-200a-3p inhibitor to determine the role of miR-200a-3p in hPDLSC osteogenesis. The capacity of generating calcium nodules and mineralised matrix is a crucial indicator of

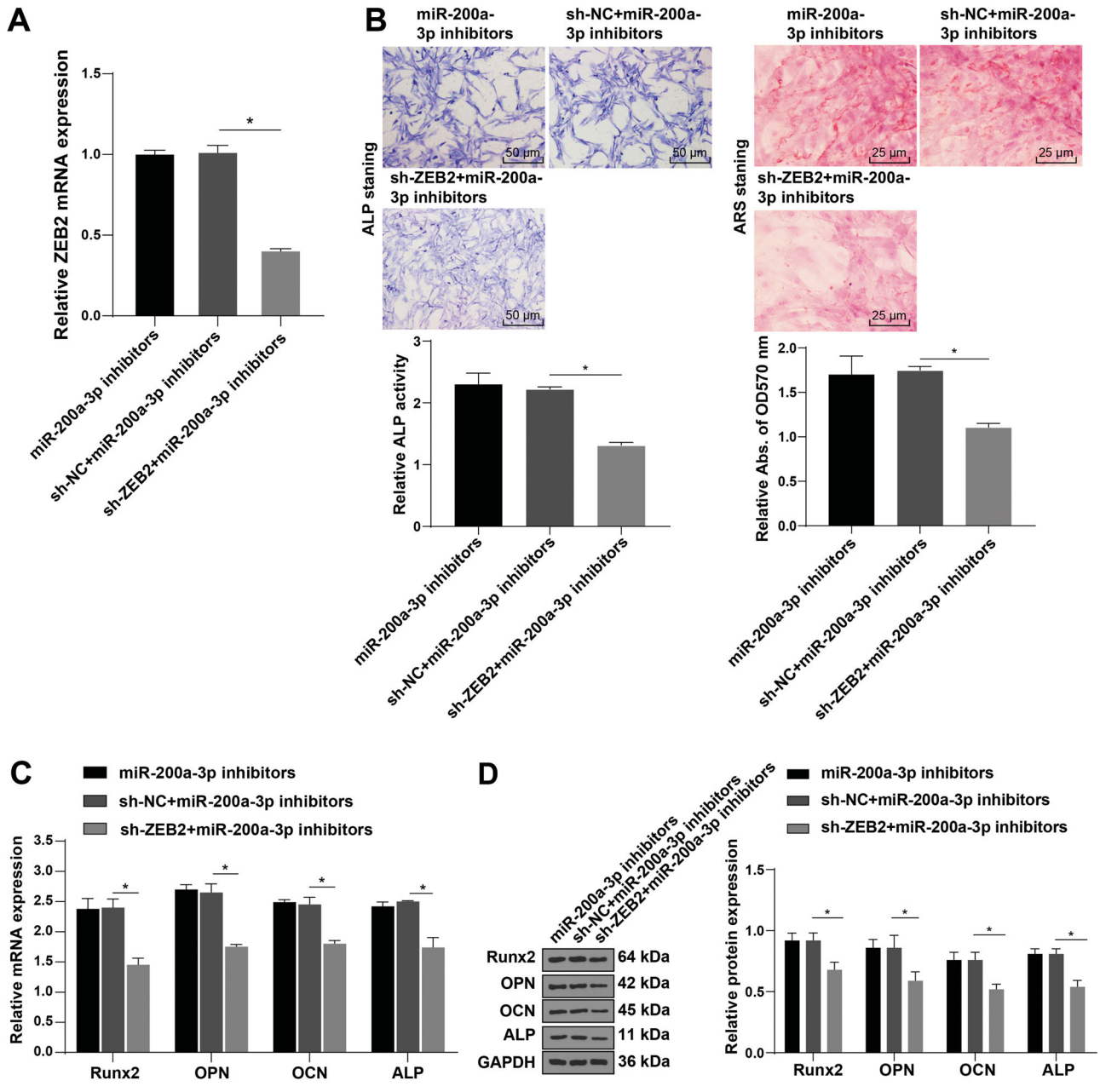

Figure 4. miR-200a-3p inhibited osteogenesis of hPDLSCs by targeting ZEB2. hPDLSCs in the miR-200a-3p inhibitor group were infected with sh-ZEB2. A: The mRNA level of ZEB2 was detected using RT-qPCR; B: ALP activity and calcified nodules were measured using ALP staining and alizarin red staining; C-D: The levels of osteogenesis-related genes (Runx2, OPN, OCN and ALP) were detected using RT-qPCR and Western blotting. The cell experiment was repeated three times independently. Data are presented as mean ± standard deviation. Data were analysed using one-way ANOVA or two-way ANOVA, followed by Tukey's multiple comparisons test, $^{*}p < .05$.

hPDLSC osteogenesis [18]. ALP activity represents an early marker of osteogenesis and participates in the mineralisation process [19]. We exhibited that ALP activity as well as the number and volume of calcified nodules decreased significantly in miR-200a-3p mimic-transfected hPDLSCs. Osteogenic differentiation is a developmental progression where cytokines, growth factors, signal transduction pathway and miRs interact together [20]. We evaluated the levels of osteogenesis-related genes (Runx2, OPN, OCN and ALP) in hPDLSCs under different treatment. Runx2 is a major marker of the osteoblast differentiation and chondrocyte maturation [21]. OCN is viewed as a biomarker of bone formation and mineralisation [22], and OPN contributes to the bone remodelling, biomineralization and periodontal regeneration [23]. We showed that these osteogenesis-related genes were reduced in miR-200a-3p mimic-transfected hPDLSCs, while miR-200a-3p inhibitor-transfected hPDLSCs showed an opposite trend. Renfa Lv *et al.* have also indicated that miR-200a-3p suppresses osteogenesis of BMSCs by targeting glutaminase, thereby expediting the progression of osteoporosis [11]. In brief, overexpression of miR-200a-3p repressed the osteogenesis of hPDLSCs.

A previous literature has unveiled that elevated miR-200a-3p expression can induce the generation of IL-2 by

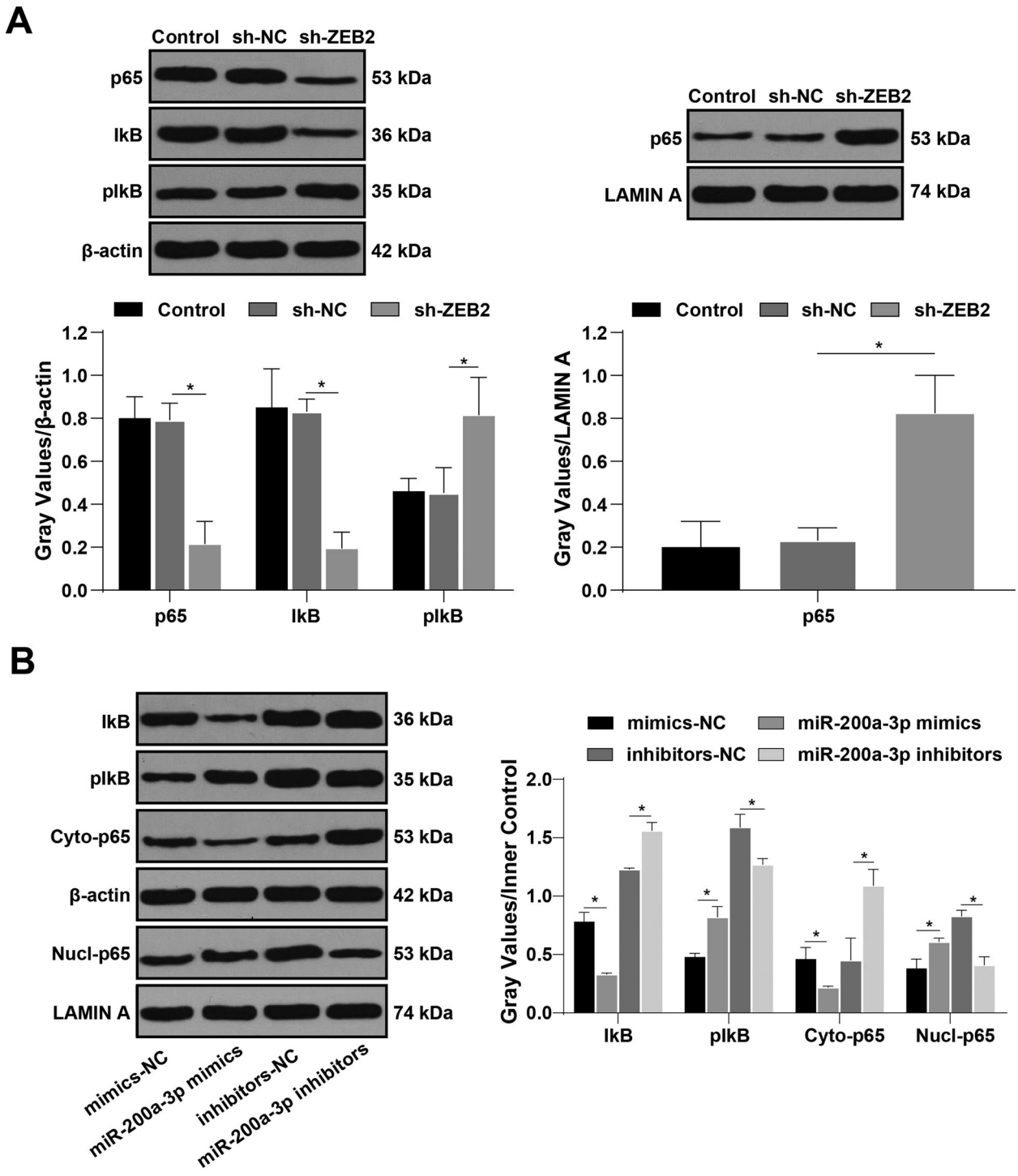

Figure 5. miR-200a-3p activated the NF-κB signalling pathway by targeting ZEB2. A/B: after intervention of ZEB2 or *miR-200a-3p*, the key proteins of the NF-κB pathway in cytoplasm and nucleus were detected using Western blotting. The cell experiment was repeated three times independently. Data are presented as mean ± standard deviation and analysed using one-way ANOVA or two-way ANOVA, followed by Tukey's multiple comparisons test, $^{*}p < .05$.

downregulating ZEB1/ZEB2 in a mouse model of systemic lupus erythematosus [24]. To explore the molecular mechanism of miR-200a-3p in the osteogenesis of hPDLSCs, we adopted bioinformatics software to analyse the target genes binding to miR-200a-3p. The targeting relationship between miR-200a-3p and ZEB2 was verified using dual-luciferase reporter gene assay. ZEB2 is a transcription factor consisting of multiple functional domains that interact with transcriptional co-effectors [25]. ZEB2 can modulate the critical transcriptional networks that are essential for cell differentiation, maintenance and function [26]. ZEB2 expression was reduced in miR-200a-3p mimic-transfected hPDLSCs but promoted in miR-200a-3p inhibitor-transfected hPDLSCs, which was suggested that miR-200a-3p targeted ZEB2 in hPDLSCs. Repression of miR-200a-3p facilitates epithelial-to-mesenchymal transition of bladder cancer cells by targeting ZEB1/ZEB2 [27]. Then, we determined the role of ZEB2 in osteogenesis of hPDLSCs. We transfected hPDLSCs with sh-ZEB2 and

found that ALP activity, calcified nodules and osteogenesis-related genes were notably reduced in sh-ZEB2-transfected hPDLSCs. Fan *et al.* have shown that downregulation of ZEB2 expression may hinder the potentials of angiogenesis and osteogenesis in human umbilical vein endothelial cells [28]. Zhai *et al.* have pointed out that the osteogenic differentiation of BMSCs can be restrained by inhibiting ZEB2 expression [12]. We demonstrated that ZEB2 silencing suppressed osteogenesis of hPDLSCs. Moreover, the functional rescue experiments further confirmed that miR-200a-3p inhibited the osteogenesis of hPDLSCs by targeting ZEB2.

Thereafter, we shifted to exploring the downstream pathway of miR-200a-3p/ZEB2 regulating osteogenic differentiation of hPDLSCs. ZEB2 is reported to attenuate LPS-induced inflammation possibly by suppressing the NF-κB pathway [13]. The NF-κB pathway represents a crucial inflammation-related pathway, which is implicated in the inflammatory secretion and osteogenesis of hPDLSCs [29]. We then investigated whether miR-200a-3p could regulate the NF-κB pathway by targeting ZEB2 during osteogenic differentiation of hPDLSCs. Generally, the activation of the NF-κB pathway is manifested as phosphorylation of IκBα and transferring of p65 from cytoplasm to nucleus [30]. We showed that IκB and p65 protein levels in the cytoplasm of sh-ZEB2-infected hPDLSCs were decreased and pIκB protein level was increased, while p65 protein level in nucleus was increased. Accumulating evidences have demonstrated that inactivation of the NF-κB pathway can potently facilitate osteoblast differentiation of hPDLSCs [31–33]. It was suggested that ZEB2 silencing could activated the NF-κB pathway. Additionally, miR-200a-3p mimic-transfected hPDLSCs showed decreased IκB and p65 protein levels in cytoplasm but increased p65 in nucleus, while miR-200a-3p inhibitor-transfected hPDLSCs had the opposite trend. Briefly, these results revealed that miR-200a-3p repressed osteogenesis of hPDLSCs *via* the ZEB2/NF-κB axis.

To sum up, miR-200a-3p represses osteogenesis of hPDLSCs by targeting ZEB2 and activating the NF-κB pathway. We explored the modulation of the miR-200a-3p/ZEB2/NF-κB axis in osteogenesis of hPDLSCs from the cellular level. However, in this study, we simply proved that miR-200a-3p activated the NF-κB signal by targeting ZEB2, but did not detect the changes of inflammation level of hPDLSCs in each group. ZEB2 can reduce the inflammation of HK-2 cells induced by lipopolysaccharide through the NF-κB pathway [13]. LIPUS can inhibit the expression of inflammatory factors by inhibiting the NF-κB pathway, and promote the osteogenic differentiation of hPDLCs [29]. Therefore, the study of LPS stimuli will be critical to demonstrate how miR-200a-3p regulates PDLSCs osteogenesis under inflammation and can better clarify the regulation mechanism of the miR-200a-3p/ZEB2/NF-κB axis in the osteogenic differentiation of hPDLCs. In addition, the animal and clinical experiments are also necessary to further verify our results. Additionally, whether the miR-200a-3p/ZEB2/NF-κB axis can be employed as a breakthrough point for periodontal tissue regeneration therapy needs further study.

Disclosure statement

The authors declare that they have no conflicts of interest.

Funding

This study was supported by the Natural Science Foundation of Guangdong Province [Grant No. 2015A030313861]. The funding body did not participate in the design of the study and collection, analysis, and interpretation of data and in writing the manuscript.

ORCID

Hui Xiao http://orcid.org/0000-0002-4209-2084

Data availability statement

All the data generated or analysed during this study are included in this published article.

References

[1] Tomokiyo A, Wada N, Maeda H. Periodontal ligament stem cells: regenerative potency in periodontium. Stem Cells Dev. 2019;28(15):974–985.
[2] Trubiani O, Pizzicannella J, Caputi S, et al. Periodontal ligament stem cells: current knowledge and future perspectives. Stem Cells Dev. 2019;28(15):995–1003.
[3] Seo BM, Miura M, Gronthos S, et al. Investigation of multipotent postnatal stem cells from human periodontal ligament. Lancet. 2004;364(9429):149–155.
[4] Son H, Jeon M, Choi HJ, et al. Decellularized human periodontal ligament for periodontium regeneration. PLoS One. 2019;14(8):e0221236.
[5] Wang J, Liu S, Li J, et al. Roles for miRNAs in osteogenic differentiation of bone marrow mesenchymal stem cells. Stem Cell Res Ther. 2019;10(1):197.
[6] Qiu W, Wu B-L, Fang F-C. Overview of noncoding RNAs involved in the osteogenic differentiation of periodontal ligament stem cells. World J Stem Cells. 2020;12(4):251–265.
[7] Xue N, Qi L, Zhang G, et al. miRNA-125b regulates osteogenic differentiation of periodontal ligament cells through NKIRAS2/NF-κB Pathway . Cell Physiol Biochem. 2018;48(4):1771–1781.
[8] Wei F, Yang S, Guo Q, et al. MicroRNA-21 regulates osteogenic differentiation of periodontal ligament stem cells by targeting Smad5. Sci Rep. 2017;7(1):16608.
[9] Feng X, Wang Z, Fillmore R, et al. MiR-200, a new star miRNA in human cancer. Cancer Lett. 2014;344(2):166–173.
[10] Wang L, Liu J, Wang Q, et al. MicroRNA-200a-3p mediates neuroprotection in Alzheimer-related deficits and attenuates amyloid-beta overproduction and tau hyperphosphorylation via coregulating BACE1 and PRKACB. Front Pharmacol. 2019;10:806.
[11] Lv R, Pan X, Song L, et al. MicroRNA-200a-3p accelerates the progression of osteoporosis by targeting glutaminase to inhibit osteogenic differentiation of bone marrow mesenchymal stem cells. Biomed Pharmacother. 2019;116:108960.
[12] Zhai Z, Chen W, Hu Q, et al. High glucose inhibits osteogenic differentiation of bone marrow mesenchymal stem cells via regulating miR-493-5p/ZEB2 signalling. J Biochem. 2020;167(6):613–621.
[13] Ding Q, Wang Y, Zhang AL, et al. ZEB2 attenuates LPS-Induced inflammation by the NF-κB pathway in HK-2 cells. Inflammation. 2018;41(2):722–731.
[14] Kato T, Hattori K, Deguchi T, et al. Osteogenic potential of rat stromal cells derived from periodontal ligament. J Tissue Eng Regen Med. 2011;5(10):798–805.

[15] Li X, Yang H, Zhang Z, et al. Platelet-rich fibrin exudate promotes the proliferation and osteogenic differentiation of human periodontal ligament cells in vitro. Mol Med Rep. 2018;18(5): 4477–4485.
[16] Ge Y, Li J, Hao Y, et al. MicroRNA-543 functions as an osteogenesis promoter in human periodontal ligament-derived stem cells by inhibiting transducer of ERBB2, 2. J Periodontal Res. 2018; 53(5):832–841.
[17] Zhang KK, Geng YD, Wang SB, et al. [MicroRNA-26a-5p targets Wnt5a to regulate osteogenic differentiation of human periodontal ligament stem cell from inflammatory microenvironment]. Zhonghua Kou Qiang Yi Xue Za Zhi. 2019;54(10):662–669.
[18] Vitale-Brovarone C, Verne E, Robiglio L, et al. Development of glass-ceramic scaffolds for bone tissue engineering: characterisation, proliferation of human osteoblasts and nodule formation. Acta Biomater. 2007;3(2):199–208.
[19] Jiang Z, Hua Y. Hydrogen sulfide promotes osteogenic differentiation of human periodontal ligament cells via p38-MAPK signaling pathway under proper tension stimulation. Arch Oral Biol. 2016;72:8–13.
[20] Moghaddam T, Neshati Z. Role of microRNAs in osteogenesis of stem cells. J Cell Biochem. 2019;120(8):14136–14155.
[21] Komori T. Runx2, an inducer of osteoblast and chondrocyte differentiation. Histochem Cell Biol. 2018;149(4):313–323.
[22] Neve A, Corrado A, Cantatore FP. Osteocalcin: skeletal and extra-skeletal effects. J Cell Physiol. 2013;228(6):1149–1153.
[23] Singh A, Gill G, Kaur H, et al. Role of osteopontin in bone remodeling and orthodontic tooth movement: a review. Prog Orthod. 2018;19(1):18.
[24] Katsuyama E, Yan M, Watanabe KS, et al. Downregulation of miR-200a-3p, targeting CtBP2 complex, is involved in the hypoproduction of IL-2 in systemic lupus Erythematosus-Derived T cells. J Immunol. 2017;198(11):4268–4276.
[25] Hegarty SV, Sullivan AM, O'Keeffe GW. Zeb2: a multifunctional regulator of nervous system development. Prog Neurobiol. 2015; 132(:81–95.
[26] Scott CL, Omilusik KD. ZEBs: Novel players in immune cell development and function. Trends Immunol. 2019;40(5):431–446.
[27] Chen W, Jiang T, Mao H, et al. SNHG16 regulates invasion and migration of bladder cancer through induction of epithelial-to-mesenchymal transition. Hum Cell. 2020;33(3):737–749.
[28] Fan X, Teng Y, Ye Z. The effect of gap junction-mediated transfer of miR-200b on osteogenesis and angiogenesis in a co-culture of MSCs and HUVECs. J Cell Sci. 2018;131(13):jcs216135.
[29] Liu S, Zhou M, Li J, et al. LIPUS inhibited the expression of inflammatory factors and promoted the osteogenic differentiation capacity of hPDLCs by inhibiting the NF-κB signaling pathway. J Periodontal Res. 2020;55(1):125–140.
[30] Manna SK. Double-edged sword effect of biochanin to inhibit nuclear factor kappaB: suppression of serine/threonine and tyrosine kinases. Biochem Pharmacol. 2012;83(10):1383–1392.
[31] Chen J, Yu M, Li X, et al. Progranulin promotes osteogenic differentiation of human periodontal ligament stem cells via tumor necrosis factor receptors to inhibit TNF-α sensitized NF-kB and activate ERK/JNK signaling. J Periodontal Res. 2020;55(3):363–373.
[32] Duan Y, An W, Wu H, et al. Salvianolic acid C attenuates LPS-induced inflammation and apoptosis in human periodontal ligament stem cells via toll-like receptors 4 (TLR4)/nuclear factor kappa B (NF-κB) pathway. Med Sci Monit. 2019;25(:9499–9508.
[33] Xu Y, Wang Y, Pang X, et al. Potassium dihydrogen phosphate promotes the proliferation and differentiation of human periodontal ligament stem cells via nuclear factor kappa B pathway. Exp Cell Res. 2019;384(1):111593.